

# Boundary induced phase transition with stochastic entrance and exit

Mithun Kumar Mitra<sup>1</sup> and Sakuntala Chatterjee<sup>2</sup>

<sup>1</sup> *Department of Physics, Indian Institute of Technology - Bombay, Powai, Mumbai 400076, India*

<sup>2</sup> *Department of Theoretical Sciences,*

*S. N. Bose National Centre for Basic Sciences,*

*Block - JD, Sector - III, Salt Lake, Kolkata 700098, India*

Abstract: We study an open-chain totally asymmetric exclusion process (TASEP) with stochastic gates present at the two boundaries. The gating dynamics has been modeled keeping the physical system of ion-channel gating in mind. These gates can randomly switch between an open state and a closed state. In the open state, the gates are highly permeable such that any particle arriving at the gate immediately passes through. In the closed state, a particle gets trapped at the gate and cannot pass through until the gate switches open again. We calculate the phase-diagram of the system and find important and non-trivial differences with the phase-diagram of a regular open-chain TASEP. In particular, depending on switching rates of the two gates, the system may or may not admit a maximal current phase. Our analytic calculation within mean-field theory captures the main qualitative features of our Monte Carlo simulation results. We also perform a refined mean-field calculation where the correlations at the boundaries are taken into account. This theory shows significantly better quantitative agreement with our simulation results.

## I. INTRODUCTION

The totally asymmetric simple exclusion process (TASEP) is a paradigmatic model for driven diffusive systems [1]. TASEP is particularly used for modeling transport in a wide variety of nonequilibrium systems, e.g. motion of molecular motors on microtubules [2–4], filamentous fungal growth [5–7] and flow of traffic on a road [8–11]. The model is defined on a one dimensional lattice on which hardcore particles perform biased diffusion. Despite its simplicity, this model shows interesting properties like the existence of a phase transition in

one dimension, which are hallmarks of nonequilibrium systems [12, 13].

One widely-studied variant of the TASEP is defined on an open lattice where in addition to performing biased diffusion, the system can also exchange particles with the reservoirs at the boundaries. In this open system, particles are injected at one end and extracted at the other end of the lattice and by tuning these injection and extraction rates one finds that the system shows a boundary induced phase transition [14–16]. The resulting phase diagram was derived using exact calculations and an alternative simpler derivation was also presented using mean field theory [14]. The phase diagram consists of a high density phase, a low density phase and a maximal current phase. As the names suggest, the high density (low density) phase is characterized by a large (small) bulk density and the maximal current phase by the presence of largest admissible current in the system.

The open chain TASEP is widely used to model transport in complex biological systems [17, 18]. Owing to the inherent complexity of a biological system, transport processes are generally coupled with other biochemical reactions. At the entry and exit terminals other reactions can take place whose outcome may influence the injection and exit processes strongly. Such a situation was considered in [19] where the species of particles undergoing transport were assumed to take part in other reactions before or after the transport *i.e.* entrance or exit are possible only when certain reactions take place. The system was modeled as an open-chain TASEP with stochastically mediated entrance or exit, facilitated by gates present at the boundaries. The opening and closing of the gate at the exit (entrance) terminal is determined by the binding and unbinding of certain receptor (initiator) to the gate. When the receptor (initiator) is bound to the gate, the particles can pass through the gate and exit (enter) the channel. When the gate at the exit (entrance) end is not bound to any receptor (initiator), it is assumed to be in a closed state when no particle can pass through. One important component in this model is the two-way coupling between the gate dynamics and the particle flow. When a particle passes through an open gate, the receptor (initiator) immediately unbinds, *i.e.* the particles ‘close the gate behind them’. The new phase diagram for this model was studied using Monte Carlo simulations and mean-field theory.

One physical system, where stochastic gates are explicitly present and control cellular transport, can be found in ion-channels, which are embedded on cell membrane and exchange of ions between cells takes place through these channels [20]. An ion-channel stochastically

switches between ‘open’ and ‘closed’ conformations and while the open conformation allows fast passage of ions through the channel resulting in a large ion-flux, no transport is possible in the closed state [21, 22]. The closed state is also known as the high-affinity state, when the ions strongly bind to the channel and hence gets trapped. In the open conformation, the channel is in the low-affinity state and the ions immediately dissociate from the channel and move to the cell cytosol.

In this paper, we explicitly model the gating dynamics, following the modeling strategy used to describe ion-channel gating [23, 24], and study its effect on the transport. We consider a generalization of an open chain TASEP, where the injection and extraction processes at the two boundaries are controlled by the presence of gates or special boundary sites, which can stochastically switch between high- and low-affinity states, as described above. While in the high-affinity state, a particle gets trapped in the gate, in the low-affinity state it immediately dissociates from the gate and moves towards right.

Our Monte Carlo simulations show that the inclusion of the above gating mechanism produces interesting and non-trivial modifications in the phase diagram. The residence time of the gates in the open state are important parameters here and depending on their value all three phases may or may not be observed. For example, unlike in ordinary TASEP, sufficiently large values of the injection and exit rates do not always yield an MC phase — the residence time of the gates in the open state must exceed certain critical values for MC phase to be observed. To explain these results we perform analytical calculations within mean-field theory. A simple mean-field theory where all correlations in the system are ignored, shows qualitative agreement with the simulation results but there is significant quantitative mismatch. To improve the quantitative agreement, we use a refined mean-field theory, developed in [7], where important correlations at the boundaries are taken into account and this approach yields better agreement with the simulation data.

In the next section we briefly summarize earlier results on the phase diagram for an ordinary open chain TASEP and then introduce our stochastic gated model in detail. In section III, we present the results of Monte Carlo simulation of our model. Our analytical calculations within simple and refined mean-field theory are presented in sections IV and V, respectively. Discussion and conclusions are presented in section VI.

## II. DESCRIPTION OF THE MODEL

The usual open-chain TASEP is defined on a one dimensional open lattice of  $L$  sites. At each site there can be at most one particle which can hop towards right, if the right neighboring site is empty. Particles are injected and extracted at the two ends of the lattice. If site 1 is empty, then a particle is injected into this site with probability  $\alpha$ . If a particle is present at site  $L$  then it exits the system with probability  $\beta$ . By varying  $\alpha$  and  $\beta$ , the following phase diagram is obtained in steady state. For  $\alpha < \beta$  and  $\alpha < \frac{1}{2}$ , the system is in a low-density (LD) phase with a bulk density  $\alpha$  and current  $J = \alpha(1 - \alpha)$ . For  $\alpha > \beta$  and  $\beta < \frac{1}{2}$  the system is in a high density (HD) phase when the bulk properties are controlled by the exit conditions. In this phase one has bulk density  $1 - \beta$  and current  $J = \beta(1 - \beta)$ . For  $\alpha = \beta < \frac{1}{2}$ , the system is in a coexistence phase when part of the system has a bulk density  $\alpha$  and the remaining part has bulk density  $(1 - \beta)$ . These two parts are connected by a domain wall or shock. The  $\alpha = \beta$  line is known as the coexistence line which terminates at  $(\alpha, \beta) = (\frac{1}{2}, \frac{1}{2})$ . For  $\alpha, \beta > \frac{1}{2}$ , the system is in a maximal current (MC) phase with bulk density  $\frac{1}{2}$ , and current  $J = \frac{1}{4}$ . This phase diagram was derived exactly in [14].

In this paper, we consider a variant of the above system, where two stochastic gates are present at the two boundary sites 1 and  $L$ . The gating dynamics is modeled so as to mimic ion-channel gating—these gates can stochastically switch between high-affinity (closed) and low-affinity (open) states. The configuration of the system is specified by specifying the occupancy of each site and the state of the gates at the boundaries. If the gate at site 1 is in the closed or high-affinity state, then the injected particle strongly binds to the site and therefore remains trapped in that site. If the gate is in the open or low-affinity state, then the particle immediately dissociates from site 1 and hops to the next site if it is empty. Similarly, if the gate at site  $L$  is closed, then a particle arriving at that site gets trapped. But if the gate is open then the particle exits the system with probability  $\beta$ . Because of the hard core constraint, no particle can enter the gate if it is already occupied. These moves are shown schematically in Fig. 1. The switching rate of the gates are assumed to follow local detailed balance. If  $p_a$  is the probability that the left gate is open, then the ratio of the forward and reverse transition rates between the open and closed states is  $(1 - p_a)/p_a$ . For the right gate the probability to be in open state is denoted by  $p_b$  and the switching rates are chosen following similar local detailed balance. We are interested in how the  $\alpha - \beta$

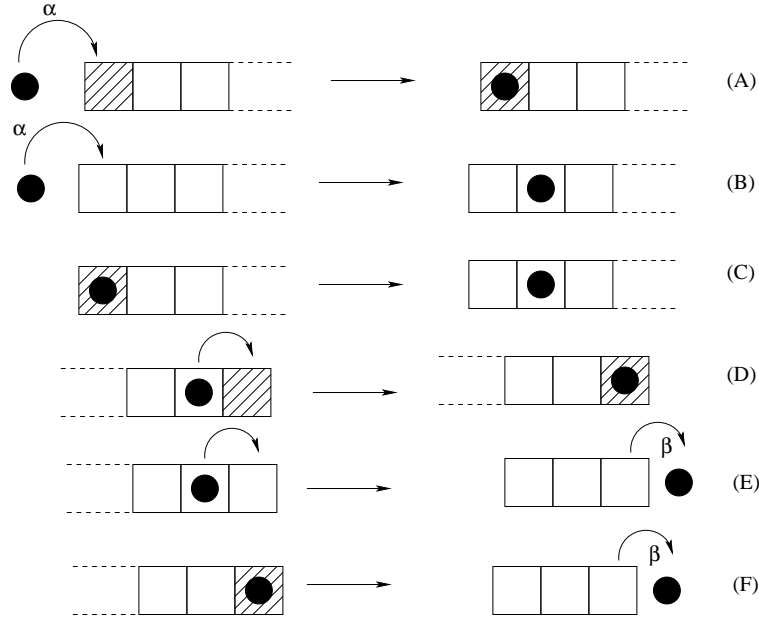


FIG. 1: Schematic representation of the moves close to the boundaries. The sites are shown as boxes and particles as black solid circles. A closed gate is shown as a shaded box at the boundary. (A): Left gate is empty and in the closed state, particle injected with probability  $\alpha$  remains trapped at site 1. (B): Left gate is empty and in the open state, particle injected with probability  $\alpha$  immediately detaches from site 1 and hops to site 2. (C): Left gate is closed and occupied, switches to an open state with probability  $p_a$  and the particle is immediately untrapped and hops to site 2. (D): Right gate is closed and empty, particle hopping from site  $L - 1$  to  $L$ , gets trapped at site  $L$ . (E): Right gate is open and empty, particle hops from site  $L - 1$  to  $L$  and after hopping immediately dissociates from site  $L$  and exits the system with probability  $\beta$ . (F): Right gate is closed and occupied, switches to an open state with probability  $p_b$  when the trapped particle immediately dissociates and exits the system with probability  $\beta$ .

phase diagram is modified for different choices of  $p_a$  and  $p_b$ .

One important point to note here is that even in the limit  $p_a = p_b = 1$ , *i.e.* when the gates are always in the open state, our model does not map onto regular open-chain TASEP. Since the gating dynamics in our system is motivated by the models for ion-channel gating [23, 24], an open state or low-affinity state of the gate implies that any particle arriving at the gate immediately detaches and goes to the next site, as shown in Fig. 1B [23, 24]. This effect is not present for a regular TASEP where the waiting time at the boundary sites is decided according to the rules of usual stochastic update. However, we have verified that

all our qualitative conclusions remain valid when we consider a variant of our model which maps onto regular TASEP in  $p_a = p_b = 1$  limit. In this modified version, a particle gets trapped in a closed gate as before, and it is allowed to leave while the gate is open, but it does not immediately dissociate from an open gate. The waiting time of a particle at the open gate is same as that at any other site. We have performed Monte Carlo simulations and analytical calculations within mean-field theory in this model and find similar results. See appendix B for more details.

### III. MONTE CARLO SIMULATIONS

We perform Monte Carlo simulations of the above model. Starting from a random initial configuration, we evolve the system in time following random sequential updates where we choose a site at random and update it following the steps outlined in appendix A. Each Monte Carlo step consists of  $L$  such update trials. Since we are mainly interested in the phase diagram, we use a large system-size  $L = 10^4$  in our simulations so as to avoid errors due to finite size effects which may cause significant difference close to the phase boundaries. The current and density profiles which characterize the phase of the system are measured after evolving for a long enough time to ensure that the system reaches steady state.

To map out the phase diagram, we study the variation of the steady state current  $J$  as a function of  $\beta$  for fixed  $\alpha$ . The current is obtained by measuring the average flux across a bond per unit time, averaged over a time-period of  $4 \times 10^8$  Monte Carlo steps. The measured current has an error-bar  $\simeq 5 \times 10^{-6}$  caused by statistical fluctuations. We find that for small  $\beta$  when the system is in HD phase,  $J$  increases with  $\beta$  and then saturates beyond a particular  $\beta_c$ . If the saturation value of  $J$  depends on  $\alpha$ , then  $\beta_c$  marks the transition from HD to LD phase. If the saturation current takes an  $\alpha$ -independent value  $\frac{1}{4}$  then  $\beta_c$  marks the transition between HD and MC phase. Using this method, we calculate the phase-diagram for various  $p_a$  and  $p_b$ , from the plot of  $J$  as a function of  $\beta$  for fixed  $\alpha$ . In Fig. 2 we show the data for  $J$  vs  $\beta$  for few representative values of  $\alpha$  and  $p_a, p_b$ .

From the  $J$  vs  $\beta$  data we obtain  $\alpha$  vs  $\beta_c$  coexistence line for each given set of  $p_a$  and  $p_b$ . In Fig. 3 we plot these coexistence lines. The critical values of  $\alpha$  and  $\beta$  that describe this phase boundary have an error-bar of 0.01 which comes from the resolution of our measurement. For  $p_a = p_b = 0.9$  and  $p_a = p_b = 0.6$  the coexistence line terminates at a particular point

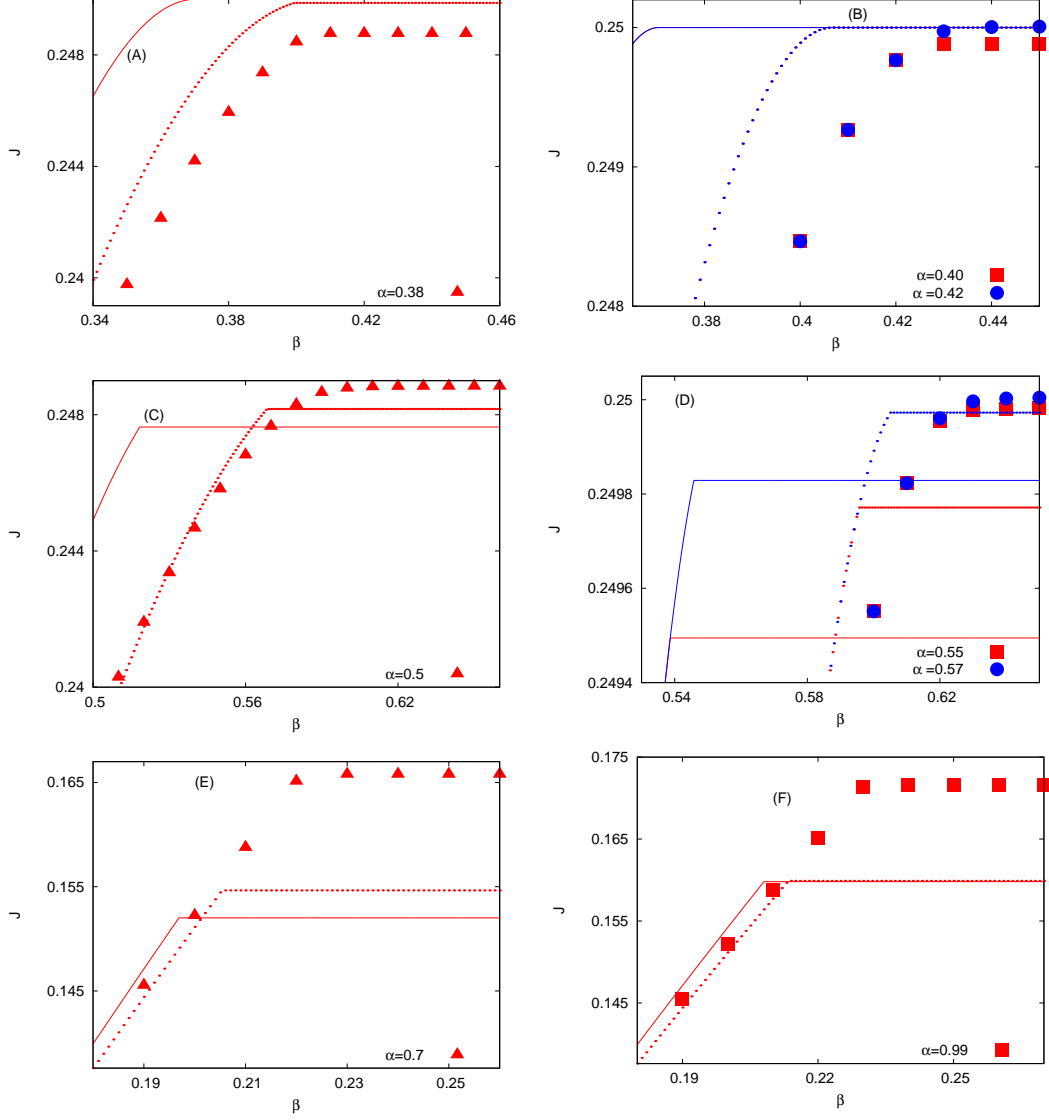


FIG. 2: Steady state current  $J$  vs exit probability  $\beta$  for fixed values of  $\alpha$  and  $p_a, p_b$ . Discrete points show simulation results, solid (dotted) continuous lines show analytical predictions from mean-field (refined mean-field) theory. Top panel:  $p_a = 0.9$ ,  $p_b = 0.9$ . (A): HD-LD transition at  $\alpha = 0.38$ ,  $\beta_c = 0.41$  (simulation) and 0.40 (refined mean-field). Mean-field predicts HD-MC transition at  $\beta_c = 0.37$ . (B): simulation shows that for  $\alpha = 0.4$  (0.42), HD-LD (HD-MC) transition at  $\beta_c = 0.43$  (0.44). For both these  $\alpha$  values, mean-field (refined mean-field) theory predicts HD-MC transition at  $\beta_c = 0.37$  (0.41). Middle panel:  $p_a = 0.6$ ,  $p_b = 0.6$ . (C): HD-LD transition for  $\alpha = 0.5$  with  $\beta_c = 0.59$  (simulation), 0.52 (mean-field) and 0.57 (refined mean-field). (D): HD-LD transition at  $\alpha = 0.55$  and  $\beta_c = 0.63$  (simulation), 0.54 (mean-field), 0.59 (refined mean-field). For  $\alpha = 0.57$  simulations show an HD-MC transition at  $\beta_c = 0.63$ . But mean-field and refined mean-field predict HD-LD transition at  $\beta_c = 0.55$  and 0.6, respectively. Bottom panel:  $p_a = 0.2$ ,  $p_b = 0.8$ . (E): HD-LD transition at  $\alpha = 0.7$ ,  $\beta_c = 0.23$  (simulation), 0.197 (mean-field), 0.205 (refined mean-field). (F): HD-LD transition at  $\alpha = 0.99$ ,  $\beta_c = 0.24$  (simulation), 0.208 (mean-field) and 0.213 (refined

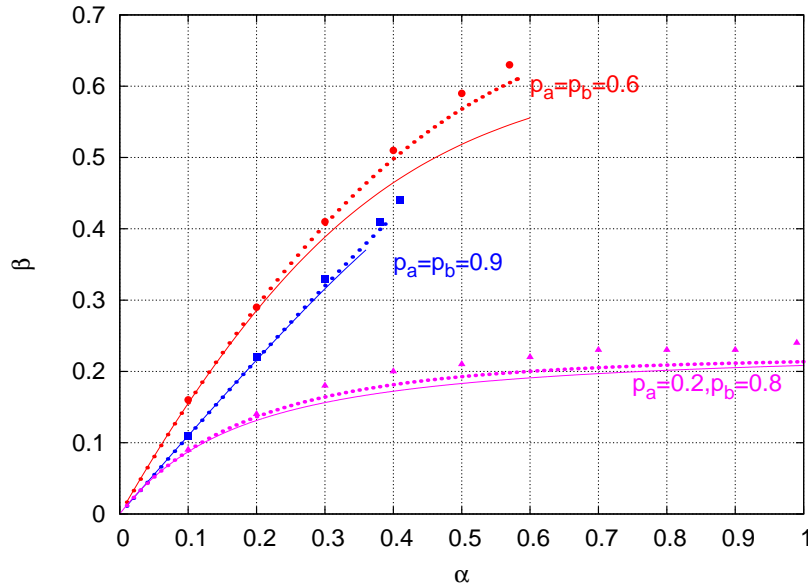


FIG. 3: Coexistence line between the HD and LD phase shown in  $\alpha - \beta$  plane for different values of  $p_a$  and  $p_b$ . Continuous lines and dotted lines show analytical predictions from simple mean-field theory and refined mean-field theory, respectively. The simulation results are shown by discrete points. The refined mean-field approach significantly improves the quantitative agreement with simulation.

and the MC phase begins. But for  $p_a = 0.2$  and  $p_b = 0.8$ , there is no MC phase, and for any  $\alpha$  in the entire range  $0 \leq \alpha \leq 1$ , one can find a  $\beta_c$  that marks the HD-LD phase transition. Hence for this case, the coexistence line extends all the way upto  $\alpha = 1$ . In the following section, we derive these results analytically using a mean-field theoretic approach.

#### IV. MEAN-FIELD THEORY

Let  $n_i$  be the occupancy of the  $i$ -th site in a particular configuration. Within simple mean-field theory we assume all correlations of the type  $\langle n_i n_j \rangle$  are factorized and can be written as  $\rho_i \rho_j$ , where  $\rho_i = \langle n_i \rangle$  is the average density at the  $i$ -th site. The time-evolution



equations for these densities are

$$\frac{\partial \rho_1}{\partial t} = \alpha(1 - p_a)(1 - \rho_1) + \alpha p_a(1 - \rho_1)\rho_2 - p_a\rho_1(1 - \rho_2) \quad (1)$$

$$\frac{\partial \rho_2}{\partial t} = p_a\rho_1(1 - \rho_2) + \alpha p_a(1 - \rho_1)(1 - \rho_2) - \rho_2(1 - \rho_3) \quad (2)$$

$$\frac{\partial \rho_i}{\partial t} = \rho_{i-1}(1 - \rho_i) - \rho_i(1 - \rho_{i+1}) \quad 3 \leq i \leq L - 1 \quad (3)$$

$$\frac{\partial \rho_L}{\partial t} = \rho_{L-1}(1 - \rho_L)(1 - \beta p_b) - p_b\beta\rho_L \quad (4)$$

Here, the first two terms on the right-hand-side of Eq. 1 represent the possible mechanisms that lead to the increase of the density at the first site—the first term corresponds to the case when the left gate is closed and an injected particle gets trapped in site 1 (as shown in Fig. 1A), the second term stands for the case when the left gate is open but the injected particle cannot immediately detach from site 1 and hop to site 2 because site 2 is already occupied. The last term in that equation describes the situation shown in Fig. 1C, when the left gate switches from closed to open state and the trapped particle is released and goes to site 2. In this way, all the terms in the above set of equations can be explained. Although we have a total of four control parameters  $\alpha, \beta, p_a$  and  $p_b$ , from the time-evolution equations it follows that  $\beta$  and  $p_b$  always appear in a product. So we treat  $\beta p_b$  as a single independent parameter.

Note that, as mentioned earlier, even when  $p_a = p_b = 1$ , these equations are not identical to those in regular open-chain TASEP. Consider the example shown in Fig. 1B, the site 2 can directly receive a particle from the reservoir when the left gate is open. Thus in the time-evolution equation for  $\rho_2$  there is a term that couples to  $\alpha$ . No such term is present for regular open-chain TASEP. Similarly, at the right boundary, the time-evolution equation for  $\rho_L$  has in general a different form even when  $p_b = 1$ . But here one can retrieve the limit for regular TASEP by redefining the exit probability as  $\beta \rightarrow \beta p_b / (1 - \beta p_b)$ .

In the steady state, all time derivatives on the left-hand-side of the equations (1)-(4) become zero and a constant current  $J$  flows through every bond in the lattice. At the left end of the system, the injection current, *i.e.* the rate of influx from the reservoir to site 1 is  $J = \alpha(1 - \rho_1)$ . Depending on the state of the gate at site 1 and on the occupancy of site 2, a fraction of the injected particles stays at site 1 and the remaining fraction immediately dissociates from site 1 and hops to site 2. Thus, the current flowing through the bond between site 1 and 2 is given by  $J = \alpha p_a(1 - \rho_1)(1 - \rho_2) + p_a(1 - \rho_2)$ . We can now construct

the following set of steady state equations, by recognizing that the current  $J$  has the same value through all the bonds of the system in the steady state.

$$\rho_1 = 1 - \frac{J}{\alpha} \quad (5)$$

$$\rho_2 = 1 - \frac{J}{p_a(1 + J - \frac{J}{\alpha})} \quad (6)$$

$$\rho_i = 1 - \frac{J}{\rho_{i-1}} \quad 3 \leq i \leq L \quad (7)$$

$$\rho_L = \frac{J}{\beta p_b} - J. \quad (8)$$

Note that for  $3 \leq i \leq L$ , the local density  $\rho_i$  satisfies the recursive relation in Eq. 7. Let the two fixed points of the recursive map be given by  $\rho_{\pm}$ , defined as  $\rho_{\pm} = (1 \pm \sqrt{1 - 4J})/2$ . It is easy to see that  $\rho_+$  is the stable fixed point and  $\rho_-$  is the unstable fixed point of the map. Also,  $\rho_+ + \rho_- = 1$  and  $\rho_+\rho_- = J$ . Below we identify different phases and the phase-boundaries following the same steps as in [14].

### A. LD Phase

In this phase, the bulk density is infinitesimally close to the unstable fixed point  $\rho_-$  and deviates from this value close to the right boundary, while satisfying  $\rho_L < \rho_+$ . Note that due to presence of the stochastic gate at site 1, the starting point of the recursive map is  $\rho_2$ , instead of  $\rho_1$ , unlike ordinary TASEP. Putting  $\rho_2 = \rho_-$  yields

$$\rho_- = 1 - \frac{J}{p_a(\rho_1 + J)} = 1 - \frac{J}{p_a(J + 1 - \frac{J}{\alpha})} \quad (9)$$

Using the relation between  $\rho_+$  and  $\rho_-$ , one gets a quadratic equation for  $\rho_-$ :

$$\rho_-^2(1 - \frac{1}{\alpha}) + \rho_-(\frac{1}{p_a} + \frac{1}{\alpha} - 1) - 1 = 0 \quad (10)$$

This has the solution

$$\rho_- = \frac{1}{2} + \frac{\alpha}{2p_a(1 - \alpha)} \mp \frac{\alpha}{2(1 - \alpha)} \left[ \left(3 - \frac{1}{\alpha}\right)^2 + \left(\frac{1}{p_a} - 1\right)^2 + \frac{2}{\alpha p_a} - 5 \right]^{1/2} \quad (11)$$

Now, by definition,  $\rho_- < 1/2$ , and since the second term in the above equation is always positive for  $0 < \alpha < 1$ , one must take the negative root and in addition one must satisfy

$$\frac{1}{p_a} < \left[ \left(3 - \frac{1}{\alpha}\right)^2 + \left(\frac{1}{p_a} - 1\right)^2 + \frac{2}{\alpha p_a} - 5 \right]^{1/2} \quad (12)$$

which after simplification gives the condition

$$(\alpha - 1)\left(5\alpha - \frac{2\alpha}{p_a} - 1\right) > 0. \quad (13)$$

Since  $0 < \alpha < 1$ , above inequality is satisfied if

$$\alpha < \frac{1}{5 - \frac{2}{p_a}} = \alpha_m, \quad 5 - \frac{2}{p_a} > 0 \quad (14)$$

For  $(5 - 2/p_a) < 0$ , i.e. for  $p_a < 2/5$ , the inequality Eq. (13) holds for all  $\alpha$ . As shown later, this implies that for  $p_a < 2/5$  there is no MC phase in the system.

### B. HD phase

In this phase, the density at the bulk and the right end is infinitesimally close to the stable fixed point  $\rho_+$  and close to the left boundary there is deviation from this value, with  $\rho_2 > \rho_-$ . Using  $\rho_L = \rho_+$  gives

$$\rho_+ = 1 - \rho_- = \frac{1 - 2\beta p_b}{1 - \beta p_b} \quad (15)$$

The condition  $\rho_+ > 1/2$  implies

$$\beta < \frac{1}{3p_b} = \beta_m \quad (16)$$

### C. MC phase

In this phase,  $\rho_2 \geq 1/2$  and  $\rho_L \leq 1/2$ . The current  $J$  takes the maximal value  $J = 1/4$  and the bulk density is  $1/2$ . From conditions specified by Eqs. (6) and (8) this phase can be observed if

$$\alpha > \alpha_m = \frac{1}{5 - \frac{2}{p_a}}; \quad \beta > \beta_m = \frac{1}{3p_b} \quad (17)$$

Since both  $\alpha$  and  $\beta$  must be less than unity, MC phase can be observed if and only if  $p_a > 1/2$  and  $p_b > 1/3$ . For  $p_a$  or  $p_b$  lower than these limiting values MC phase does not exist. Note that this takes care of the condition  $p_a > 2/5$  derived in Eq. 14.

### D. HD-LD Coexistence line

On the critical line separating HD and LD phase, we match the expression for  $\rho_- = 1 - \rho_+$  obtained from Eqs. (11) and (15) for the two phases:

$$\frac{1}{2} + \frac{\alpha}{2p_a(1-\alpha)} - \frac{\alpha}{2(1-\alpha)} \left[ \left(3 - \frac{1}{\alpha}\right)^2 + \left(\frac{1}{p_a} - 1\right)^2 + \frac{2}{\alpha p_a} - 5 \right]^{1/2} = \frac{\beta p_b}{1 - \beta p_b} \quad (18)$$

This is the equation for the coexistence line which terminates at  $\alpha = \alpha_m$  and  $\beta = \beta_m$  and MC phase starts from this point. It follows from this equation that when the gates are always open, *i.e.*  $p_a = p_b = 1$ , then the coexistence line is given by  $\alpha = \beta$ , as in regular TASEP, but it terminates at  $\alpha_m = \beta_m = 1/3$ , instead of  $\alpha_m = \beta_m = 1/2$ . However, for general values of  $p_a$  and  $p_b$ , the coexistence line has a curvature.

We compare the coexistence line obtained from mean-field theory (continuous lines) with that from simulation (discrete closed symbols) in Fig. 3. We find that there is good qualitative agreement between the two but there is a systematic quantitative deviation. For example, at  $p_a = 0.2$ ,  $p_b = 0.8$ , our simulation shows there is no MC phase and this is consistent with the criterion derived in section IV C. However, mean-field systematically under-estimates  $\beta_c$  values for all  $\alpha$  and the mismatch becomes more prominent for large  $\alpha$  values. This also affects the MC phase boundaries. For  $p_a = p_b = 0.9$ , mean-field predicts that the coexistence line should terminate at  $\alpha_m = \frac{9}{25} = 0.36$  and  $\beta_m = \frac{10}{27} \simeq 0.37$ . But our simulation gives  $\alpha_m = 0.41$  and  $\beta_m = 0.44$ . Similarly, for  $p_a = p_b = 0.6$ , mean-field prediction is  $\alpha_m = \frac{3}{5} = 0.6$  and  $\beta_m = \frac{5}{9} \simeq 0.56$ , whereas our simulation yields  $\alpha_m = 0.57$  and  $\beta_m = 0.63$ . Thus there is significant mismatch between the mean-field and simulation results. To improve the quantitative agreement with simulations, we develop a refined mean-field theory in the next section.

### V. REFINED MEAN FIELD THEORY

Unlike the simple mean field theory described above, where all correlations between the sites are ignored, in this refined mean-field approach, we take into account certain correlations in the system, which are expected to be more important than others, in a self-consistent way, as was first demonstrated in a model for a dynamically extending exclusion process [7]. In the bulk of the system one still expects the correlations to be weak. But

close to the boundary this assumption breaks down and strong correlations may be present between the sites. For example, in the limit of small  $p_a$  when the residence time of the left gate in the closed state is large, an injected particle remains trapped at site 1 for long enough such that the particle at site 2 (if any) has time to drift away towards the bulk of the system before the gate opens. When the gate opens finally, the trapped particle hops to site 2. Therefore, for small values of  $p_a$ , a strong anti-correlation develops between sites 1 and 2. For general values of  $p_a, \alpha$  and  $\beta$ , depending on the interplay of the time-scales associated with boundary injection, exit and switching process of the left gate, the correlation between the sites 1 and 2 can become positive or negative and vary in strength. Similarly, at the right boundary a correlation develops between sites  $L - 1$  and  $L$ .

Let  $C_a = \langle n_1 n_2 \rangle$  and  $C_b = \langle n_{L-1} n_L \rangle$  be the correlation between the sites near the left and right boundary, respectively. Unlike simple mean-field theory, we do not replace these correlations by simple product, rather we treat  $C_a$  and  $C_b$  as additional variables. All other correlations in the system are assumed to be factorized. Therefore, the equations of motion are:

$$\frac{\partial \rho_1}{\partial t} = \alpha(1 - p_a)(1 - \rho_1) + \alpha p_a(\rho_2 - C_a) - p_a(\rho_1 - C_a) \quad (19)$$

$$\frac{\partial \rho_2}{\partial t} = p_a(\rho_1 - C_a) + \alpha p_a(1 - \rho_1 - \rho_2 + C_a) - \rho_2(1 - \rho_3) \quad (20)$$

$$\frac{\partial C_a}{\partial t} = \alpha(\rho_2 - C_a) - C_a(1 - \rho_3) \quad (21)$$

$$\frac{\partial \rho_i}{\partial t} = \rho_{i-1}(1 - \rho_i) - \rho_i(1 - \rho_{i+1}) \quad 3 \leq i \leq L - 2 \quad (22)$$

$$\frac{\partial \rho_{L-1}}{\partial t} = \rho_{L-2}(1 - \rho_{L-1}) - \rho_{L-1} + C_b \quad (23)$$

$$\frac{\partial \rho_L}{\partial t} = (\rho_{L-1} - C_b)(1 - \beta p_b) - p_b \beta \rho_L \quad (24)$$

$$\frac{\partial C_b}{\partial t} = \rho_{L-2}(\rho_L - C_b) - \beta p_b C_b \quad (25)$$

In steady state, when all time-derivatives vanish, we express  $C_a, \rho_1, \rho_3$  in Eqs 19 and 21 in terms of  $\rho_2$  and  $J$  to obtain the following equation

$$\alpha p_a \rho_2^2 + \alpha \rho_2 \left( J - p_a + \frac{p_a J}{\alpha} \right) + J \left[ J(1 - p_a) - p_a \left( 1 - \frac{J}{\alpha} \right) \right] = 0 \quad (26)$$

For a given  $J$  the above quadratic equation can be solved for  $\rho_2$ :

$$\rho_2 = \frac{1}{2} - \frac{J}{2} \left( \frac{1}{p_a} + \frac{1}{\alpha} \right) \pm \frac{1}{2\alpha p_a} \sqrt{\alpha^2 \left( J - p_a + \frac{p_a J}{\alpha} \right)^2 - 4\alpha p_a J \left[ J(1 - p_a) - p_a \left( 1 - \frac{J}{\alpha} \right) \right]} \quad (27)$$

From here, one can work out the conditions for the MC phase, where  $J = 1/4$  and  $\rho_2 \geq 1/2$ . The last criterion implies that in Eq. 27 only positive root should be taken and one must have

$$\alpha^2 \left( J - p_a + \frac{p_a J}{\alpha} \right)^2 - 4\alpha p_a J \left[ J(1 - p_a) - p_a \left( 1 - \frac{J}{\alpha} \right) \right] \geq (\alpha J + p_a J)^2 \quad (28)$$

For  $J = 1/4$  in MC phase this condition gives

$$\alpha^2 \left( p_a^2 - \frac{p_a}{2} \right) + \frac{\alpha}{4} (3p_a^2 - p_a) - \frac{p_a^2}{4} \geq 0 \quad (29)$$

This is the condition that must be satisfied at the left boundary of the chain to observe MC phase. To work out the condition for the right boundary, we consider Eqs. 23, 24 and 25 from where we replace  $\rho_L$ ,  $\rho_{L-2}$  and  $C_b$  in terms of  $\rho_{L-1}$  and  $J$  to obtain the following equation.

$$\beta^2 p_b^2 \rho_{L-1}^2 - \beta p_b (J + \beta p_b + \beta p_b J) \rho_{L-1} + J(J + \beta p_b) = 0 \quad (30)$$

For a given  $J$  this equation can be solved for  $\rho_{L-1}$

$$\rho_{L-1} = \frac{1}{2} + \frac{J}{2} \left( 1 + \frac{1}{\beta p_b} \right) \pm \frac{1}{2\beta p_b} \sqrt{(J + \beta p_b + \beta p_b J)^2 - 4J(J + \beta^2 p_b^2)} \quad (31)$$

from which negative root must be taken since in MC phase  $\rho_{L-1} \leq 1/2$ . In addition, one must satisfy

$$\frac{1}{2\beta p_b} \sqrt{(J + \beta p_b + \beta p_b J)^2 - 4J(J + \beta^2 p_b^2)} \geq \frac{J}{2} \left( 1 + \frac{1}{\beta p_b} \right) \quad (32)$$

and for  $J = 1/4$  this gives

$$\beta \geq \frac{\sqrt{3} - 1}{2p_b} \quad (33)$$

Eqs. 29 and 33 define the conditions that must be satisfied in order for the system to support an MC phase.

The HD-LD coexistence line can be obtained from matching the solutions of Eqs. 26 and 30. For example, in Eq. 30 we use the conditions for HD phase and substitute  $\rho_{L-1} = \rho_+$  and  $J = \rho_+(1 - \rho_+)$  to obtain

$$\rho_+^2 + \rho_+(\beta^2 p_b^2 + \beta p_b - 2) + 1 - \beta p_b - \beta^2 p_b^2 = 0 \quad (34)$$

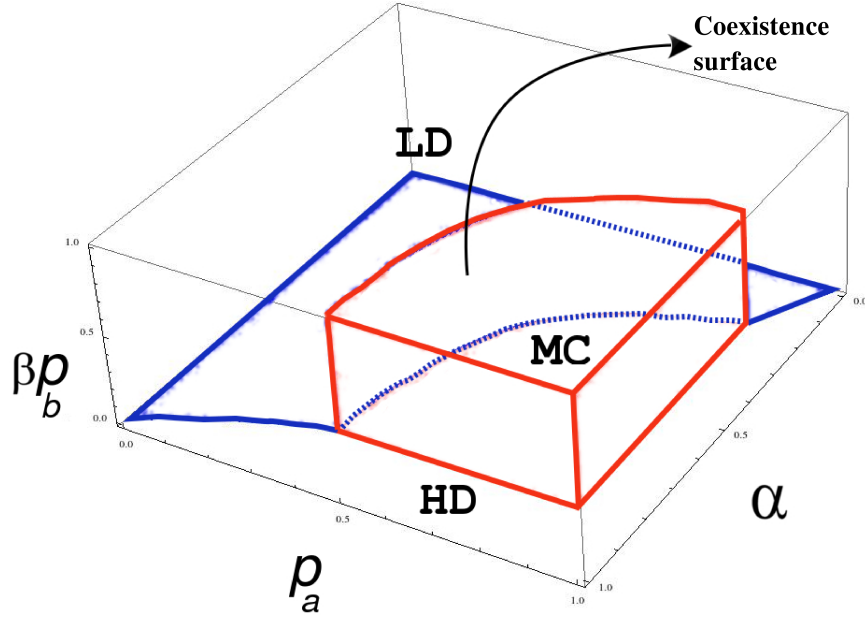


FIG. 4: Complete phase diagram in three dimensions obtained from refined mean-field theory with control parameters  $\alpha$ ,  $p_a$  and  $\beta p_b$ . The coexistence surface is the one demarcated by the thick blue lines. The region enclosed by the thick red lines indicates the maximal current phase. The region above the coexistence surface is the low-density phase, while the region below the coexistence surface is the high-density phase.

which has a solution

$$\rho_+ = 1 - \beta p_b - \beta^2 p_b^2 \quad (35)$$

and another trivial solution  $\rho_+ = 1$  which we neglect. Since  $\rho_+ > 1/2$ , one must have  $\beta p_b(1 + \beta p_b) < 1/2$  for HD phase, which is consistent with the criterion obtained in Eq. 33.

For LD phase we use Eq. 26 and substitute  $\rho_2 = \rho_-$  and  $J = \rho_-(1 - \rho_-)$  to obtain the following cubic equation

$$\rho_-^3 \left(1 - p_a + \frac{p_a}{\alpha}\right) + \rho_-^2 \left(p_a - \frac{2p_a}{\alpha} - \alpha - 2\right) + \rho_- \left(\alpha p_a + \alpha + p_a + \frac{p_a}{\alpha} + 1\right) - (\alpha p_a + p_a) = 0 \quad (36)$$

The solution for  $\rho_-$  obtained from this equation must match that obtained in Eq. 35 on the HD-LD coexistence line. Therefore, the equation for coexistence line is obtained by substituting  $\rho_- = \beta p_b(1 + \beta p_b)$  in Eq. 36.

In Fig. 2 we show variation of  $J$  with  $\beta$  (dotted lines) for different  $p_a, p_b$  values. The

critical point  $\beta_c$  is the value of  $\beta$  for which the current  $J$  reaches a saturation. As can be seen from the figure, refined mean field theory consistently predicts a more accurate value for  $\beta_c$  as compared to mean field theory. The actual value of the current is also predicted better by the refined mean field theory. The remaining discrepancy between the theory and simulation results may be attributed to the presence of non-zero correlations extending into the bulk, beyond the first and last site correlations taken into account in our refined mean-field approach. In Fig. 3 we plot the coexistence line (dotted line) from refined mean-field theory and compare with the simulation results. Even in this case we find that compared to simple mean-field, the refined mean-field prediction shows a better quantitative agreement with simulation results. In Fig. 4 we present the complete phase diagram in three dimension with the three independent parameters,  $\alpha$ ,  $p_a$  and  $\beta p_b$  as axes. The coexistence region (Eq. 36) is a surface in this three dimensional space, as shown in Fig. 4.

## VI. CONCLUSION

In this paper, we have studied the phase diagram of an open-chain TASEP whose entrance and exit at the boundaries are controlled by two gates, whose dynamics are chosen so as to mimic ion-channel gates in cell membrane. In our model, these gates can switch between a high-affinity state, when it strongly binds to the particles thereby trapping them, and a low-affinity state, when particle immediately dissociates from the gates and move to the next site. This immediate dissociation implies even in the limit when the gates are always open, our model does not map onto a regular open-chain TASEP. However, all our results and conclusions remain valid in a slightly different version of the model, where there is no immediate dissociation in the open state (see appendix B) and usual TASEP limit is recovered, when the gates are always open.

The effect of stochastic gates on the phase diagram was studied earlier where a two-way coupling between the gating dynamics and particle flow was considered [19]. While entrance of exit of particles can take place only through an open gate, immediately after passage the gate shuts close. On the other hand, in our model, no such two-way coupling is assumed and the gates can switch between two states, completely independent of the particle flow. Even this uncoupled, independent gating dynamics yields important modification in the phase diagram which cannot be reproduced by mere rescaling of entrance and exit rates.



Stochastic gating, as investigated in our model, allows systems to actively control the phase diagram, and hence the current flow through the lattice, independent of the entry and exit rates. The entry and exit rates often depend on the concentration of particles near the boundary sites, and gating then allows a mechanism for systems to prevent flow even in the presence of high concentrations (or equivalently, high entry rate) and vice versa. This opens new possibilities for mechanisms for the regulation of particle current, especially in biological systems. It might be of interest to include more biologically relevant features in our model and check how generic our present results are.

### Acknowledgments

MKM would like to acknowledge support from the Ramanujan Fellowship (RJN-09/2012), Department of Science and Technology, India and the IRCC Seed Grant from IIT-Bombay.

### Appendix A: Simulation Algorithm

We evolve the system following random sequential update where a randomly chosen site is updated according to the steps outlined below.

- (a) Choose an integer  $k$  within  $[0, L]$ .
- (b) If  $1 < k < L - 1$ , then a particle hops from site  $k$  to  $k + 1$ , if the  $k$ -th site is occupied and  $(k + 1)$ -th site is empty.
- (c) If  $k = L - 1$ , and if  $(L - 1)$ -th site is occupied and  $L$ -th site is empty, a particle hops from  $L - 1$  to  $L$ . After the hopping takes place, the particle attempts to exit the system with probability  $\beta$ , if the gate at site  $L$  is open. If the hopping attempt is unsuccessful, the particle stays at site  $L$ .
- (d) If  $k = 0$ , then if site 1 is empty, a particle is injected into site 1 with probability  $\alpha$ . If the gate at site 1 is open, the injected particle immediately hops to site 2, if site 2 is empty.
- (e) If  $k=1$ , and if the gate at site 1 is open, close it with probability  $1 - p_a$ . If the gate is closed, open it with probability  $p_a$  and if there is a particle, it hops to site 2, if site 2 is empty.
- (f) If  $k = L$  and if the gate at site  $L$  is open, close it with probability  $1 - p_b$ . If the gate is closed, open it with probability  $p_b$  and after opening the gate, the particle at site  $L$ , if

any, attempts to exit the system with probability  $\beta$ .

### Appendix B: Open state without immediate dissociation

In this section, we discuss a variant of our model that maps onto the regular open-chain TASEP in the limit when the gates are always open. The only difference between this model and the one discussed in the main part of the paper is that in the open state of the gate there is no immediate dissociation. In other words, the hopping rate of a particle from an open gate is same as the hopping rate from any bulk site (as opposed to an infinite hopping rate that stands for immediate dissociation). The mean-field equations for this system read

$$\frac{\partial \rho_1}{\partial t} = \alpha(1 - \rho_1) - p_a \rho_1(1 - \rho_2) \quad (\text{B-1})$$

$$\frac{\partial \rho_2}{\partial t} = p_a \rho_1(1 - \rho_2) - \rho_2(1 - \rho_3) \quad (\text{B-2})$$

$$\frac{\partial \rho_i}{\partial t} = \rho_{i-1}(1 - \rho_i) - \rho_i(1 - \rho_{i+1}) \quad 3 \leq i \leq L - 1 \quad (\text{B-3})$$

$$\frac{\partial \rho_L}{\partial t} = \rho_{L-1}(1 - \rho_L) - \beta p_b \rho_L \quad (\text{B-4})$$

It is easy to see that in the limit  $p_a = p_b = 1$  this model maps onto regular open-chain TASEP.

Following the method illustrated in section IV these equations can be solved to derive the following equation for the coexistence line

$$1 + \frac{\alpha}{p_a} - \left[ \left( 1 + \frac{\alpha}{p_a} \right)^2 - 4\alpha \right]^{1/2} = 2\beta p_b \quad (\text{B-5})$$

which terminates at  $\alpha_m = \frac{1}{2(2 - 1/p_a)}$  and  $\beta_m = \frac{1}{2p_b}$  and MC phase starts from here. The coexistence line obtained from simulation (data not shown) matches qualitatively with this calculation but there is a quantitative mismatch. This is taken care of when refined mean-field theory is used. Following the steps outlined in section V, it is easy to show that within refined mean-field theory the equation for the coexistence line becomes

$$\alpha \beta^2 p_b^2 - \beta p_b (1 + \alpha - \beta p_b) \left[ 1 - \beta p_b (1 - \beta p_b) \left( \frac{1}{\alpha} + \frac{1}{p_a} \right) \right] = 0 \quad (\text{B-6})$$

This line shows much better quantitative agreement with the simulation (data not presented

here).

- 
- [1] G.M. Schütz and K.J. Wiese, *Phase transitions and critical phenomena* **19** 1 (2001).
  - [2] Y. Aghababaie, G.I. Menon and M. Plischke, *Phys. Rev. E* **59** 2578 (1999)
  - [3] R. Lipowsky, S. Klumpp and T.M. Nieuwenhuizen, *Phys. Rev. Lett.* **87** 108101 (2001).
  - [4] S. Klumpp and R. Lipowsky, *J. Stat. Phys.* **113** 233 (2003).
  - [5] K.E.P. Sugden, M.R. Evans, W.C.K. Poon and N.D. Read, *Phys. Rev. E* **75** 1909 (2007).
  - [6] M.R. Evans and K.E.P. Sugden *Physica A* **384** 53 (2007)
  - [7] K.E.P. Sugden and M.R. Evans, *J. Stat. Mech.* P11013 (2007).
  - [8] D. Chowdhury, D.E. Woif and M. Schreckenberg, *Physica A* **235** 417 (1997).
  - [9] D. Chowdhury, L. Santen and A. Schadschneider *Phys. Rep.* **329** 199 (2000)
  - [10] D. Helbing, *Reviews of Modern Physics* **73** 1067 (2001).
  - [11] H.J. Hilhorst and C. Appert-Rolland, *J. Stat. Mech.* P06009 (2012).
  - [12] J. Krug, *Phys. Rev. Lett.* **67** 1882 (1991).
  - [13] M. Henkel and G. Schütz, *Physica A* **206** 187 (1994).
  - [14] B. Derrida, E. Domany and D. Mukamel, *J. Stat. Phys.* **69** 667 (1992).
  - [15] B. Derrida, M.R. Evans, V. Hakim and V. Pasquier, *J. Phys. A: Math. Gen.* **26** 1493 (1993).
  - [16] G. Schütz and E. Domany, *J. Stat. Phys.* **72** 277 (1993).
  - [17] T. Chou, K. Mallick and R.K.P. Zia, *Rep. Prog. Phys.* bf 74 116601 (2011).
  - [18] D. Chowdhury, A. Schadschneider and K. Nishinari, *Phys. Life Rev.* **2** 318 (2005).
  - [19] A.J. Wood, *J. Phys. A: Math. Theor.* **42**, 445002 (2009).
  - [20] Hille, *B. Ionic Channels of Excitable Membranes*, Sinauer, Sunderland, MA (1992).
  - [21] E. Neher and B. Sakmann, *Nature* 260, 799802 (1976).
  - [22] A. L. Hodgkin and A. F. Huxley, *J. Physiol.* **117**, 500 (1952).
  - [23] A.M.J. VanDongen, *Proc. Nat. Acad. Sc.* **101**, 3248 (2004).
  - [24] D. Andreucci, D. Bellaveglia, E.N.M. Cirillo, and S. Marconi, *Phys. Rev. E* **84**, 021920 (2011).